



Universal approach of cellulose fibres chemical modification result analysis via commonly used techniques

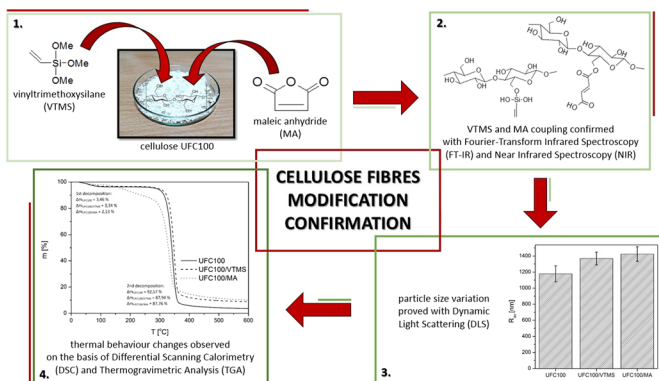
Stefan Cichosz¹ · Anna Masek¹ · Korneliusz Wolski¹ · Marian Zaborski¹

Received: 3 April 2018 / Revised: 13 August 2018 / Accepted: 16 August 2018 /
Published online: 20 August 2018
© The Author(s) 2018

Abstract

This article considers the modification of cellulose fibres with the use of vinyltrimethoxysilane and maleic anhydride as substances to improve the wettability of the additive in the hydrophobic polymer matrix. The stress is put on the possible ways of modification impact investigation and its description. Effects of the treatment are analysed using Fourier transform infrared spectroscopy, which reveal the presence of new moieties on the cellulose surface, e.g. C=C bonds, C=O and Si–C groups, while dynamic light scattering investigation revealed an increase in the hydrodynamic radii of the molecules which was maximized in the case of modification with the use of maleic anhydride. Furthermore, thermal properties were defined with differential scanning calorimetry and thermogravimetric analysis. Some variations within the process of samples thermal degradation are observed—thermal stability of the specimen modified with maleic anhydride is the highest. The presented approach of combined fibre modification analysis techniques, being a scientific novelty, allows to confirm the treatment impact on cellulose properties at many levels.

Graphical abstract



Keywords Cellulose · Maleic anhydride · Vinyltrimethoxysilane

Extended author information available on the last page of the article

Introduction

Increasing interest in new materials from renewable resources and potentially environmental friendly methods for modifying such materials has led to increased interest in using cellulose [1]. Due to its abundance in the environment and its quick renewability as a biodegradable raw material [2], cellulose and its modifications have become a subject of research for many scientists. Cellulose exists in the cell walls of plants and can be produced by bacteria. It is a polysaccharide that is formed by the repeated connection of D-glucose building blocks, and it is characterized by specific properties that differ from other natural and synthetic polymers. Cellulose is distinguished by its hydrophilicity, biodegradability and broad chemical modification capacity [3]. The high hydrophilicity of the cellulose surface defines its behaviour in different media as well as its interactions with different chemicals. Adjusting the surface properties of cellulose is of great importance for its current and future applications, such as in papermaking and composites [4].

Various research papers have shown the great variety of properties that can be obtained through modifying the cellulose surface. The modification of plant fibres may involve removing the surface impurities, swelling the crystalline region and removing the hydrophilic hydroxyl groups. Effectively reinforcing composites with plant fibres depends on the moisture content, fibre–matrix interfacial adhesion [5], and crystalline and cellulose content. The alkalization of plant fibres improves their performance as a composite reinforcement [6]. Cellulose can also be chemically altered to increase its potential by making derivatives such as carboxymethyl cellulose, methyl cellulose, ethyl cellulose, hydroxypropyl cellulose and cyanoethyl cellulose [7]. Carboxymethyl cellulose (CMC) stands out among the stated derivatives; it is manufactured in significant amounts due to its wide commercial applications with regard to volume demands. It is used in many different industries, including food ingredients, pharmaceuticals and materials [8]. Such diverse applications along with its low pricing make CMC one of the major market shareholders within all the cellulose ether product categories [9].

Recently, ionic liquids (ILs) that have hydrogen bond acceptors in their structure, such as Cl^- , Br^- or SCN^- , have been used to dissolve and process cellulose with great success [10–12]. These hydrogen bond acceptors are thought to be responsible for interrupting the extensive intermolecular and intramolecular hydrogen bonding within cellulose [13–15]. Due to the structure of cellulose, it is regarded as an active chemical. Functional groups can be introduced into the cellulose molecules through the hydroxyl moieties. New groups break the hydrogen bonding network in the cellulose, decrease the crystallinity and increase its solubility [16–19]. Ionic liquids have been used as a reaction medium for modifying cellulose using urea, phthalic anhydride (PA), maleic anhydride (MA) and butyl glycidyl ether (BGE). Previous experiments have shown that the hydrogen bonding interactions decrease and that anhydride groups have a higher reaction activity with hydroxyl groups [20].

Cellulose-based materials are easily obtained and can be employed as relatively cheap absorbents. They may also be used to remove heavy metal ions prior to the appropriate chemical treatment. Chemically modified cellulose materials present

higher absorption capacities than unmodified forms. Modifications can be carried out in two ways. Monomer-grafting enables attaching many different functional groups to the backbone of cellulose. Another method of attaching new specific groups to the cellulose is direct modification in which new groups are bonded to hydroxyl groups through chemistries such as base solutions, mineral and organic acid solutions, organic compounds or oxidizing agents [21–23].

Despite development of new modification techniques, well-known compounds like silane coupling agents and various anhydrides are commonly used chemical modifiers. Due to their structure, they are able to form chemical bridges between cellulose fibres and the matrix. In various experiments, it was suggested that chemical reactions between cellulose and a coupling agent led to improvements in the mechanical properties of the composites. In spite of the fact that they are being commonly employed in cellulose modification, convincing evidence was not provided [24].

Materials

Reagents

The Arbocel[®] UFC100 Ultrafine Cellulose for Paper and Board Coating was the type of cellulose used for modification. It is in a powder form, nonmodified and insoluble in water. Simultaneously, this cellulose exhibits a high water binding capacity (even at high temperatures and shearing forces). Its average fibre length is 8 μm .

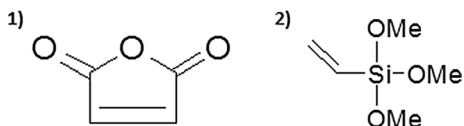
The first of the used modifiers was maleic anhydride (MA), otherwise known as 2,5-furandione, provided by Sigma-Aldrich[®]. It is a white solid substance with a molecular mass of 98.06 g/mol and is commonly used in cellulose chemical modification. When dissolved in water, it turns into maleic acid. Its melting point is somewhere in the region of 51–56 °C (lit.) or 52–54 °C. Furthermore, the fibres were also treated with vinyltrimethoxysilane (VTMS) U-611 from UniSil[®], which is a transparent, colourless liquid. In addition to being dissolvable in benzene, carbon tetrachloride and acetone environments also have the capability of reacting with water. All reagents were commercial products of the highest purity available, and their structural formulas are shown in Fig. 1.

Methods

Chemical modification

The cellulose was modified using vinyltrimethoxysilane (VTMS) and maleic anhydride (MA). In both cases, fibres were dried for 24 h at 70 °C, and then, the temperature was raised to 100 °C for an hour before performing the modification.

Fig. 1 Structural formulas of (1) maleic anhydride (MA) and (2) vinyltrimethoxysilane (VTMS)



As for the modification with maleic anhydride, the cellulose was treated in an acetone at room temperature for 2 h (oil bath 40 °C, 60 r/min) using an evaporator. After stirring, the acetone was removed with a vacuum distillation process (oil bath 60 °C, initial pressure 200 mbar). Then, the sample was heated in a vacuum oven at 100 °C and 170 mbar for 4 h [25]. Figure 2 describes the maleinization process of the cellulose fibres with the creation of ester bonds on the surface of the filler.

Modification with the use of VTMS, the ethanol (used as a solvent), cellulose and silane were stirred, with the use of a rotary evaporator, in a flask for 4 h at 60 r/min (oil bath, 40 °C). Then, the vacuum distillation (oil bath 60 °C, initial pressure 200 mbar) was performed. After removing the solvent, the samples were dried for 24 h in a vacuum oven (40 °C, 170 mbar) and then for 48 h in a dryer at 120 °C [28]. Figure 3 presents the scheme of the silanization of the cellulose fibres with a focus on the successive stages of the chemical modification.

Such prepared powders were stored in a dryer at 40 °C. In Table 1, the conditions taken into consideration during all stages of both modifications processes are provided.

Fourier transform infrared spectroscopy

Fourier transform infrared spectroscopy (FTIR) absorbance spectra have been investigated within the 4000–400 cm^{-1} range which helped in assessing structural changes as each chemical group has its specific absorption band. The experiment has been performed with the use of Thermo Scientific Nicolet 6700 FTIR spectrometer (p/n 912A0637) equipped with diamond Smart Orbit ATR sampling accessory (p/n 840-145300).

Thermogravimetric analysis

Thermogravimetric analysis (TGA) has been used in order to get acquainted with thermal degradation process detecting the mass loss as a function of raising temperature in the range from 0 to 600 °C. Mettler Toledo® TGA/DSC 1 STAR^c System equipped with Gas Controller GC10 has been employed in this investigation.

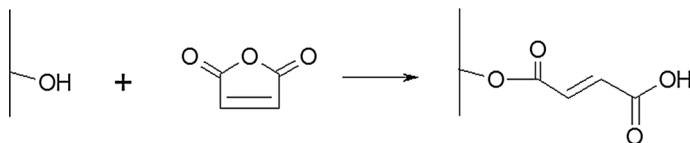


Fig. 2 Reaction scheme of the cellulose fibres with maleic anhydride [26]

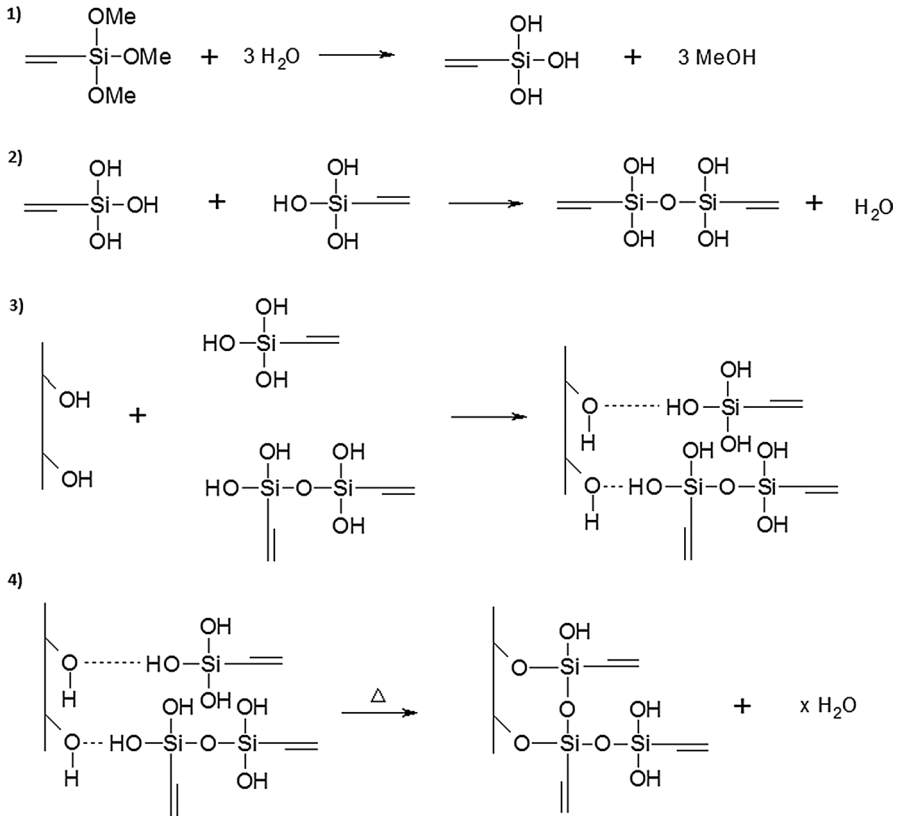


Fig. 3 Scheme of the cellulose fibre modification with VTMS: (1) hydrolysis; (2) condensation; (3) adsorption; (4) and chemical grafting [27]

On the basis of the gathered data thermal degradation steps, activation energies have been calculated with Broido [50] and Coats [51] methods in order to assess thermal stability of the prepared samples.

Table 1 Tabularized parameters of the chemical modifications in solution

Ingredients	Modification in solution	Drying process	Storage conditions
VTMS Cellulose ARBOCEL UFC100 Ethanol	Evaporator: 40 °C, 60 r/min, 4 h	I step: Vacuum oven: 24 h, 40 °C, 170 mbar II step: Dryer: 48 h, 120 °C	Dryer: 40 °C
MA Cellulose ARBOCEL UFC100 Acetone	Evaporator: 40 °C, 60 r/min, 2 h	Vacuum oven: 4 h, 100 °C, 170 mbar	

Differential scanning calorimetry

Differential scanning calorimetry (DSC) investigation has been performed in a temperature range from -50 to 300 °C prior to analyse enthalpy changes (ΔH) during thermal decomposition of cellulose. Here, as well, Mettler Toledo® TGA/DSC 1 STAR^c System equipped with Gas Controller GC10 has been employed.

Dynamic light scattering

Measurements of the particle sizes of cellulose UFC100 were taken using aqueous dispersion of the samples (0.1 g of the powder per 200 ml of distilled water). These solutions were subjected to ultrasound for 30 min, and the dispersion samples were poured into colorimetric cuvettes [29]. ZetaSizer Nano-S90 from Malvern Instruments has been employed.

Results and discussion

FTIR analysis

The vibrational spectra of the cellulose fibres exhibit observable band changes depending on the kind of modification conducted. Their analysis provides valuable information and helps to suggest the cellulose changes after maleic anhydride (MA) and vinyltrimethoxysilane (VTMS) grafting.

Considering Figs. 2, 3 and the results from other scientific studies, visible changes were observed. For the modification performed with the use of MA, the increased intensity of the absorption bands related to the C–O, C=O and C=C bonds was observed [30]. In contrast, the cellulose treated with VTMS indicated signals of the chemical groups containing silicon atoms [31, 32] and C=C bonds. In addition, in both cases, a decrease in the intensity of the absorption band of the –OH moieties was observed as a result of the creation of ester and Si–O bonds. Visible absorption bands may also have their origin from unreacted reagents adsorbed on the cellulose fibres surface.

Taking a closer look at Fig. 4, the absorption band at 3332 cm^{-1} was assigned to the O–H stretching vibrations that occurred due to both the water and O–H moiety content in the sample. The broadband in the $3600\text{--}3100\text{ cm}^{-1}$ region also provided considerable information concerning the presence of hydrogen bonds [33]. Moving further, the absorption band at 2894 cm^{-1} was connected to the C–H stretching vibrations coming from the cellulose fibres. These two peaks have been observed in many other works [34, 35]. Each of the performed modifications contributed to the decrease in the intensity of those absorption bands, compared to the initial cellulosic samples, and, thus, also to the lower concentration of the O–H and C–H moieties in these two samples.

As for the maleinization reaction of cellulose, some new signals were observed. The stretching vibration at 1719 cm^{-1} was assigned to the C=O bond [35], and

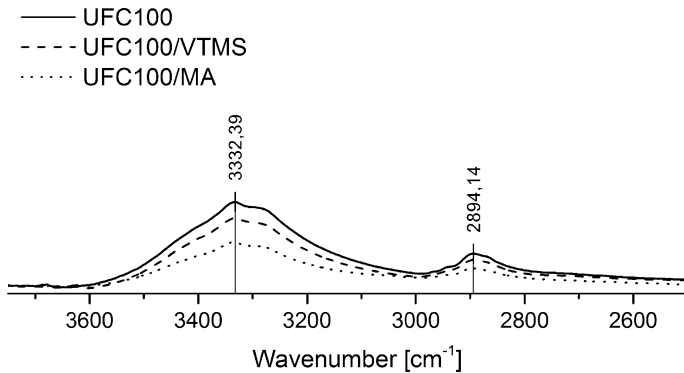


Fig. 4 FTIR spectra of the cellulose (4000–2500 cm^{-1}) and absorption bands characteristic of the cellulose fibres: 3332 cm^{-1} (O–H, adsorbed water) and 2894 cm^{-1} (C–H)

the peak in the range of 1640–1618 cm^{-1} corresponds to the aldehydic and carboxyl stretching vibrations [26] or even to the adsorbed water, which was also identified in a few other studies [36]. According to Fig. 5, the presence of those moieties confirms the occurrence of new functional groups on the cellulose fibres surface. Moreover, an increase in the intensity of the absorption in the range of 1300–1200 cm^{-1} [37] and 900–800 cm^{-1} was observed, which was due to the increased concentration of the C–H, C=O and C–O–C bonds. Nevertheless, a decrease in the intensity in the range between 1150 and 1000 cm^{-1} was observed; the 1104 cm^{-1} band was attributed to the asymmetric in-phase ring vibrations, 1030 cm^{-1} was assigned to the C–O–C vibrations, and 1046–1043 cm^{-1} was attributed to the C–C, C–O–H, C–H and side group vibrations [38].

The modification with the use of the silane coupling agent was not as easy to confirm as the maleinization reaction due to the overlapping effect of absorption bands. The absorption bands visible in Figs. 5 and 6, which correspond to the C–O and C–C stretching vibrations and CH_2 rocking vibration at 1161–895 cm^{-1} , also correspond to the Si–O–Si (1100 cm^{-1} , 950–800 cm^{-1}), Si–O–C (1450 cm^{-1}), Si–OH (~900 cm^{-1}) and C–Si–C bonds (663 cm^{-1}) [39, 40]. The phenomenon of overlapping in the case of the silanization of the cellulose fibres was also observed in previous studies [41].

However, a few shifts in the absorption bands to lower and higher wavenumbers were noted, in which comparison is shown in Fig. 7, e.g. –OH stretching vibration at 3332 cm^{-1} , C–H stretching vibration at 3894 cm^{-1} , C–O–C and side group vibrations at 897 cm^{-1} , and C–OH out-of-plane bending at 558 cm^{-1} . They could be caused by the interactions between the adsorbed and grafted silane and maleic anhydride functional groups, which are mainly polar, with infrared irradiation.

The FTIR absorption band at 1428 cm^{-1} , visible in Fig. 5, that was assigned to the symmetric CH_2 bending vibration decreased. Its intensity, in comparison with the reference sample, reflects a possible reduction in the degree of the crystallinity of the sample modified with VTMS. This phenomenon was clearly described in detail in previous studies concerning the crystalline structures of cellulose fibres [33].

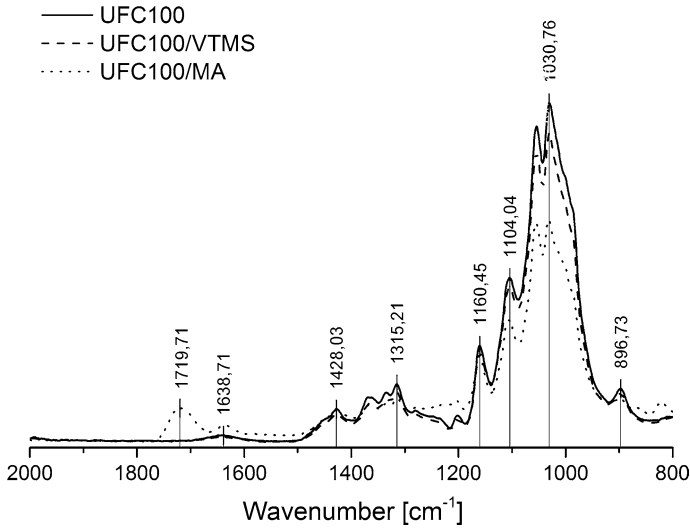


Fig. 5 FTIR spectra of the cellulose (2000–800 cm^{-1}); the visible moieties characteristic of MA: 1719 cm^{-1} , 1638 cm^{-1} (C=O), 1046–1043 cm^{-1} (C–C, C–OH, C–H) and 1030 cm^{-1} (C–O–C); and the overlapping phenomenon in the case of VTMS: 1161–895 cm^{-1} (C–C, C–O), 1110 cm^{-1} and 850–800 cm^{-1} (Si–O–Si)

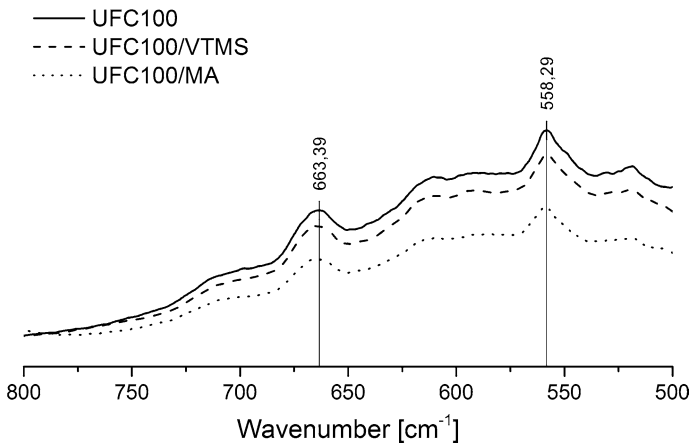


Fig. 6 FTIR spectra of the cellulose (800–500 cm^{-1}) and modification with the use of VTMS reflected by the absorption band at 663 cm^{-1} (C–Si–C)

DLS investigation

DLS analysis is a technique that can provide valuable information in order to confirm the occurrence of a modification process. It provides data regarding the hydrodynamic radii, which have been carefully described in previous studies [42, 43]. Here, the particle size changes may indicate the effect of performed treatments.

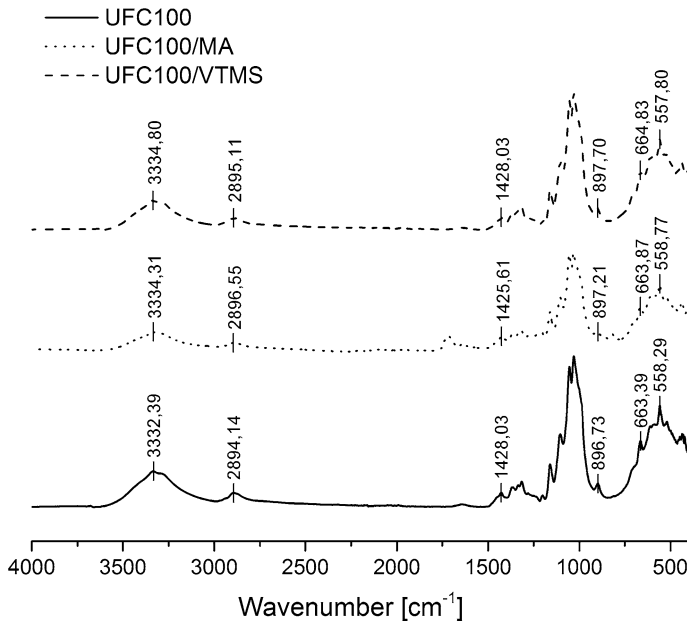


Fig. 7 Wavenumber shifts visible in the FTIR spectra that were caused by the interactions between the macromolecules

According to Table 2, it can be seen that the size of the particles changed depending on the employed modifier. The biggest particles were obtained with the use of maleic anhydride. However, in both cases, an increase in the hydrodynamic radius was observed, which proves that grafting occurred on the surface of the cellulose fibres (Fig. 8).

However, the creation of clusters and chain entanglements is possible. The influence of the concentration on these phenomena has been widely described [44]. Despite the fact that the exact radii values of the cellulose fibres might have been not known due to the aggregation processes, the results of the DLS investigation provided more details about their affinity to one another concerning the chemical groups on their surface and the surface free energy of the cellulose. The bigger are observed particles, the better affinity and possible treatment effect on particle interactions.

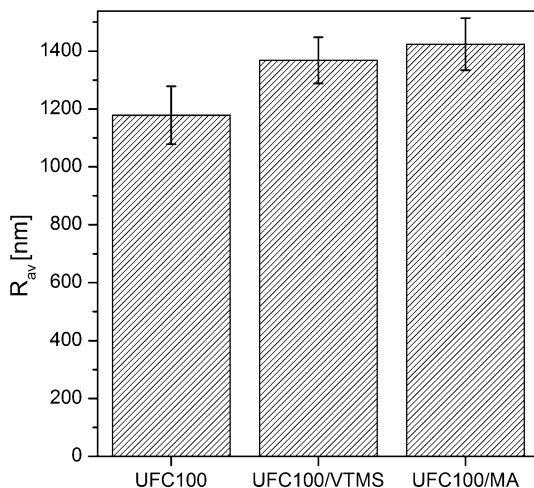
TGA analysis

A thermogravimetric investigation was conducted in order to define the changes in the thermal decomposition of the cellulose fibres. Many studies have been conducted on this topic [45, 46].

Considering Fig. 9, the first mass loss of each material was attributed to the release of water and volatile matter [47, 48] up to 150 °C. The decreases in the mass values at this stage for neat UFC100, UFC100/VTMS and UFC100/MA were

Table 2 Acute values of the cellulose fibre sizes

Sample	R_{average} (nm)
UFC100 ref.	1178
UFC100/VTMS	1364
UFC100/MA	1424

Fig. 8 Comparison of the sizes of the cellulose fibres

3.46%, 3.24% and 2.13%, respectively. The second decomposition event occurred at various temperatures with the initial point originated from 150 to 250 °C, depending on the type of modified material. This stage was assigned to the thermal degradation of the cellulose fibres [35]. As shown in Fig. 9, the mass loss is lower in the case of the cellulose modified with MA (87.76%) and VTMS (87.94%), while for the neat cellulose fibres, this value is higher and equal to 92.57%.

In Table 3, the data regarding the effects of modifying the cellulose with the silane VTMS and MA, representing the thermal stability of the materials, are shown. According to the first modifier, the thermal degradation of cellulose was prolonged but not as well as in the case of the modification with maleic anhydride. The use of MA resulted in an earlier onset of more intensive degradation and prolonged the whole process, which was determined from the tabularized temperature values.

The thermogravimetric analysis evidenced that the weight loss of the chemically modified cellulose fibres was lower than that of the unmodified sample, similar to other studies [26]. Moreover, the thermogravimetric curve of the neat UFC100 sample exhibited congruous parameters to the microcrystalline cellulose (MCC) thermogravimetric curve described by other scientists [49].

Activation energies of thermal decomposition steps have been established with Broido [50] and Coats [51] methods as it has been shown in various researches

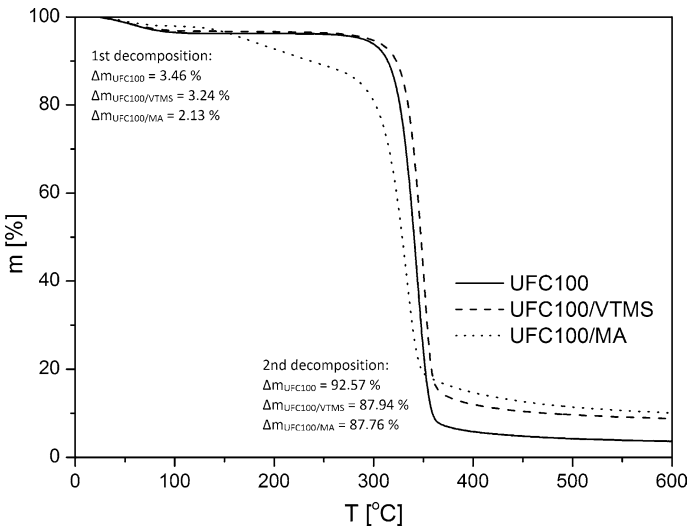


Fig. 9 TGA curves of the cellulose. The first decomposition stage is assigned to the evaporation of water and the remaining unreacted modifiers. The second mass loss is attributed to the thermal degradation of the cellulose

Table 3 Temperatures of the mass loss

Sample	$T_{5\%}$ (°C)	$T_{10\%}$ (°C)	$T_{15\%}$ (°C)	$T_{50\%}$ (°C)	$T_{90\%}$ (°C)
UFC100	289	314	322	340	359
UFC100/VTMS	295	322	330	347	472
UFC100/MA	170	236	286	329	599

$T_{x\%}$ —temperature at which the mass loss is $x\%$

[52–54]. Obtained values are in well correspondence and are confirmed in the literature [55].

According to the results presented in Table 4, it may be concluded that the lowest value of first thermal decomposition activation energy is observed in case of the sample treated with maleic anhydride which confirms previously observed significant decrease in $T_{5\%}$. UFC100/MA occurs to be the specimen of poor thermal stability.

On the other hand, modification with VTMS contributes to an increase of 1st step E_a in comparison with the reference sample. Consequently, UFC100/VTMS thermal resistance has been improved. Similar trends are observed considering 2nd decomposition step.

Table 4 Activation energies of thermal degradation steps calculated according to Broido [50] and Coats method [51]

Sample	Activation energy E_a (kJ/mol)			
	Broido method		Coats method	
UFC100	1st step	101 ± 4	1st step	103 ± 1
	2nd step	258 ± 9	2nd step	254 ± 3
UFC100/VTMS	1st step	108 ± 4	1st step	109 ± 1
	2nd step	280 ± 10	2nd step	275 ± 5
UFC100/MA	1st step	85 ± 5	1st step	81 ± 1
	2nd step	230 ± 10	2nd step	234 ± 5

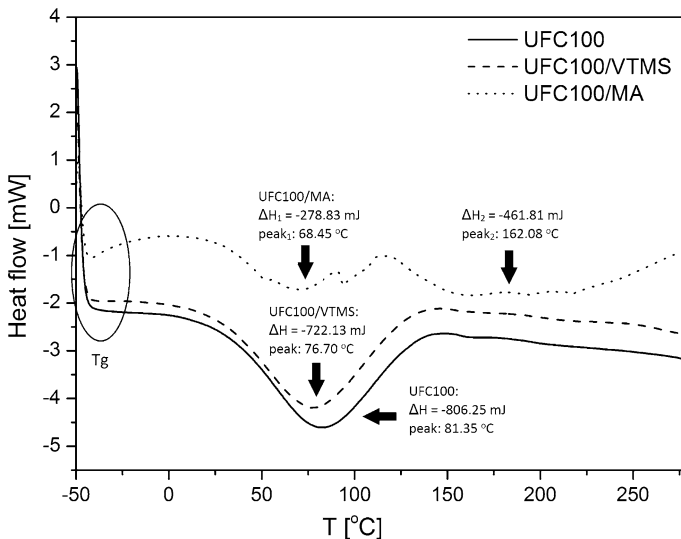


Fig. 10 DSC analysis of the cellulose samples. Visible changes during the process of evaporation of the adsorbed water and thermal decomposition of the cellulose fibres

DSC investigation

Thermograms reveal some details about the water evaporation from the cellulose surface and fibres initial thermal decomposition [56]. The DSC analysis revealed that even at 100 °C, completely dried cellulose was not obtained. These data show how troublesome it is to achieve the full desorption of water from the surface of hydrophilic fillers. This problem was also mentioned in other studies [57, 58] that evaluated the effect of water content on the glass transition temperature.

According to Fig. 10, the T_g of all samples is near the region of -40 °C, which, according to another study [59], indicates that the water content in the specimens, surprisingly, could be even approximately 17%. Nevertheless, no significant changes between the specimens, considering T_g , have been noted.

The endothermic peaks at about 80 °C were strengthened as a consequence of the evaporation of water and the inner volatile substances. The shifts in the peaks to lower temperatures of the modified samples in comparison with the reference samples should be emphasized—from 81.35 °C (UFC100 ref.) to 76.70 °C (UFC100/VTMS) and 68.45 °C (UFC100/MA). Furthermore, the changes in the enthalpy also varied. The highest value was observed in the case of the neat cellulose fibres. A similar effect was observed in another study and was described as a result of the increase in the length-to-diameter ratio during the performed modification. Therefore, according to the authors, the evaporation of moisture was facilitated [60] which contributed to the fall in enthalpy values.

In conjunction with Fig. 10, thermal degradation prolongation, in case of cellulose treated with maleic anhydride, a second endothermic peak, of a higher enthalpy value, can be observed at 162.08 °C. This may be connected with more complex thermal degradation of MA. Inasmuch as the earlier decomposition of the fibre is visible in the DSC curve, the data provide a perfect confirmation of phenomenon observed in TGA—poor thermal stability of UFC100/MA in comparison with UFC100/VTMS.

Conclusions

The samples have been characterized primarily from IR data. The FTIR spectra revealed that the chemical modification of the cellulose was successful. The absorption bands at 1719 cm^{-1} (C=O stretching vibrations) and 1638 cm^{-1} (aldehydic and carboxyl stretching vibrations) originated from the maleic anhydride grafted on the surface of the fibres. In the case of the silanization reaction, the shifts in the wavenumbers and the intensity decrease at 1428 cm^{-1} were crucial. They indicated, not only, different interactions between the functional groups of the cellulose with the adsorbed and grafted silane but also information regarding the decrease in the degree of crystallinity. Nevertheless, possible signals from unreacted modifiers observed in FTIR spectra have to be considered.

The DLS investigation proved that the modified fillers had a bigger size in comparison with unmodified sample, and the thermogravimetric analysis evidenced that the weight loss of the chemically modified cellulose fibres was lower. Moreover, the various onset times of the chemical decomposition of the inner specimens were noted and confirmed with both TGA and DSC investigations. The best improvement in thermal resistance, according to activation energy calculations, has been detected in case of VTMS treated cellulose fibres.

All things gathered, performed modifications have affected cellulose structure as well as its thermal properties. Prepared filler may be added to the polymer matrix in order to create various green composites finding application, e.g. in packaging or automotive industry, which is of a high importance considering its higher biodegradation potential. Moreover, given fibres treatment result analysis, universal approach allows to describe chemical modification impact at many levels.

Open Access This article is distributed under the terms of the Creative Commons Attribution 4.0 International License (<http://creativecommons.org/licenses/by/4.0/>), which permits unrestricted use, distribution, and reproduction in any medium, provided you give appropriate credit to the original author(s) and the source, provide a link to the Creative Commons license, and indicate if changes were made.

References

1. Rodionova G, Lenes M, Eriksen Ø, Gregersen Ø (2011) Surface chemical modification of microfibrillated cellulose: improvement of barrier properties for packaging applications. *Cellulose* 18:27–134
2. Dufresne A, Belgacem M (2013) Cellulose-reinforced composites: from micro- to nanoscale. *Polimeros* 23:277–286
3. Klemm D, Schumann D, Kramer F, Heßler N, Koth D, Sultanova B (2009) Nanocellulose materials—different cellulose, different functionality. *Macromol Symp* 280:60–71
4. Gardner D, Oporto G, Mills A, Samir M (2008) Adhesion and surface issues in cellulose and nanocellulose. *J Adhes Sci Technol* 22:545–567
5. Moushiul Alam AKM, Beg MDH, Reddy Prasad DM, Kham MR, Mina MF (2012) Structures and performances of simultaneous ultrasound and alkali treated oil palm empty fruit bunch fiber reinforced poly(lactic acid) composites. Part A. *Appl Sci Manuf* 43:1921–1929
6. Mwaikambo LY, Ansell MP (2002) Chemical modification of hemp, sisal, jute, and kapok fibres by alkalization. *J Appl Polym Sci* 84:2222–2234
7. Varshney VK, Naithani S (2011) Chemical functionalization of cellulose derived from nonconventional sources. In: Kalia S et al (eds) *Cellulose fibers: bio and nano-polymer composites*. Springer, Berlin, pp 43–60
8. Saputra AH, Qadhaiya L, Pitaloka AB (2014) Synthesis and characterization of carboxymethyl cellulose (cmc) from water hyacinth using ethanol–isobutyl alcohol mixture as the solvents. *IJCEA* 5:36–40
9. Joshi G, Naithani S, Varshney VK, Bisht SS, Rana V, Gupta PK (2015) Synthesis and characterization of carboxymethyl cellulose from office waste paper: a greener approach towards waste management. *Waste Manag* 38:33–40
10. Barthel S, Heinze T (2006) Acylation and carbanilation of cellulose in ionic liquids. *Green Chem* 8:301–306
11. Heinze T, Schwikal K, Barthel S (2005) Ionic liquids as reaction medium in cellulose functionalization. *Macromol Biosci* 5:520–525
12. Wendler F, Kosan B, Krieg M, Meister F (2009) Possibilities for the physical modification of cellulose shapes using ionic liquids. *Macromol Symp* 280:112–122
13. Edgar K, Heinze T, Liebert T (2009) *Cellulose solvents: for analysis, shaping and chemical modification*. American Chemical Society, Washington
14. Wu J, Zhang J, Zhang H, He J, Ren Q, Guo M (2004) Homogeneous acetylation of cellulose in a new ionic liquid. *Biomacromolecules* 5:266–268
15. Liu S, Sun G (2008) Radical graft functional modification of cellulose with allyl monomers: chemistry and structure characterization. *Carbohydr Polym* 71:614–625
16. Dahou W, Ghemati D, Oudia A, Aliouche D (2010) Preparation and biological characterization of cellulose graft copolymers. *Biochem Eng J* 48:187–194
17. Kamel S, Ali N, Jahangir K, Shah SM, El-Gendy AA (2008) Pharmaceutical significance of cellulose: a review. *Express Polym Lett* 2:758–778
18. Narita M, Tabata M, Yoshida A (2007) *Methods for preparing alkali cellulose and cellulose ether*. US 0149774A1
19. Odian G (2004) *Principles of polymerization*. Wiley, Hoboken
20. Zhang X, Wang F, Keer LM (2015) Influence of surface modification on the microstructure and thermo-mechanical properties of bamboo fibers. *Materials* 8:6597–6608
21. O’Connell DW, Birkinshaw C, O’Dwyer TF (2008) Heavy metal adsorbents prepared from the modification of cellulose: a review. *Bioresour Technol* 99:6709–6724
22. Wan Ngah WS, Hanafiah MALM (2008) Removal of heavy metal ions from waste water by chemically modified plant wastes as adsorbents: a review. *Bioresour Technol* 99:3935–3948

23. Hokkanen S, Bhatnagar A, Sillanpaa M (2016) A review on modification methods to cellulose-based adsorbents to improve adsorption capacity. *Water Res* 91:156–173
24. Zhou F, Cheng G, Jiang B (2014) Effect of silane treatment on microstructure of sisal fibers. *Appl Surf Sci* 292:806–812
25. Teaca CA, Bordiliau R, Spiridon I (2014) Maleic anhydride treatment of soft wood—effect on wood structure and properties. *Cellul Chem Technol* 42:863–868
26. Bodirlau R, Teaca CA (2009) Fourier transform infrared spectroscopy and thermal analysis of ligno-cellulose fillers treated with organic anhydrides. *Rom J Phys* 54:93–104
27. Yanjun X, Callum ASH, Zefang X, Holger M, Carsten M (2010) Silane coupling agents used for natural fiber/polymer composites: a review. *Composites* 41:806–819
28. Song J, Rojas OJ (2013) Approaching super-hydrophobicity from cellulosic materials: a review. *NPPRJ* 28:216–238
29. Oberlerchner JT, Rosenau T, Potthast A (2015) Overview of methods for the direct molar mass determination of cellulose. *Molecules* 20:10313–10341
30. Wibowo AC, Desai SM, Mohanty AK, Drzal LT, Misra M (2006) A solvent free graft copolymerization of maleic anhydride onto cellulose acetate butyrate bioplastic by reactive extrusion. *Macromol Mater Eng* 291:90–95
31. Hassan MM, Khan MA (2008) Role of N-(β -amino ethyl) γ -aminopropyl trimethoxy silane as coupling agent on the jute-polycarbonate composites. *Polym Plast Technol Eng* 47:847–850
32. Pacheco DM, Johnson JR, Koros WJ (2012) Aminosilane-functionalized cellulosic polymer for increased carbon dioxide sorption. *Ind Eng Chem Res* 51:503–514
33. Ciolacu D, Ciolacu F, Popa VI (2011) Amorphous cellulose—structure and characterization. *Cellul Chem Technol* 45:13–21
34. Li Y, Xiao J, Chen M, Song Z, Yi Z (2014) Adsorbents based on maleic anhydride-modified cellulose fibers/diatomite for dye removal. *J Mater Sci* 49:6696–6704
35. Zhang W, Li C, Liang M (2010) Preparation of carboxylate-functionalized cellulose via solvent-free mechanochemistry and its characterization as a biosorbent for removal of Pb^{2+} from aqueous solution. *J Hazard Mater* 181:468–473
36. Sheltami RM, Kargarzadeh H, Abdullah I (2015) Effects of silane treatment of cellulose nanocrystals on tensile properties of cellulose polyvinyl chloride nanocomposite. *Sains Malays* 44:801–810
37. Proniewicz LM, Paluszkiwicz C, Weselucha-Birczynska A, Majcherczyk H, Baranski A, Konieczna A (2001) FT-IR and FT-Raman study of hydrothermally degraded cellulose. *J Mol Struct* 596:1–3
38. Mizi F, Dasong D, Biao H (2012) Fourier transform infrared spectroscopy for natural fibres. In: Salich S (ed) *Fourier transform—materials analysis*. InTech, Rijeka
39. Thakur MK, Gupta RK, Thakur VK (2014) Surface modification of cellulose using silane coupling agent. *Carbohydr Polym* 111:849–855
40. Abdelmouleh M, Boufi S, Salah A, Belgacem MN, Gandini A (2002) Interaction of silane coupling agents with cellulose. *Langmuir* 18:3203–3208
41. Loof D, Hiller M, Oschkinat H, Koschek K (2016) Quantitative and qualitative analysis of surface modified cellulose utilizing TGA-MS. *Materials* 9:415–428
42. Oberlerchner JT, Rosenau T, Potthast A (2015) Overview of methods for the direct molar mass determination of cellulose. *Molecules* 20:10313–10341
43. Pamies R, Zhu K, Kjoniksen AL, Nystrom B (2009) Thermal response of low molecular weight poly-(N-isopropylacrylamide) polymers in aqueous solution. *Polym Bull* 62:487–502
44. Luo C, Wang S, Liu H (2007) Cellulose conversion into polyols catalysed by reversibly formed acids and supported ruthenium clusters in hot water. *Angew Chem Int Ed* 46:7636–7639
45. Das K, Ray D, Bandyopadhyay NR, Sengupta S (2010) Study of the properties of microcrystalline cellulose particles from different renewable resources by XRD, FTIR, Nanoindentation, TGA and SEM. *J Polym Environ* 18:355–363
46. Yang H, Yan R, Chen H, Lee DH, Zheng C (2007) Characteristics of hemicellulose, cellulose and lignin pyrolysis. *Fuel* 86:12–13
47. Ma S, Yu SJ, Wang ZH (2013) Ultrasound-assisted modification of beet pulp cellulose with phthalic anhydride in ionic liquid. *Cellul Chem Technol* 47:527–533
48. Wysau G, Gimba CE, Agbaji EB, Ndukwe GI (2016) Thermo-gravimetry (TGA) and DSC of thermal analysis techniques in production of active carbon from lignocellulosic materials. *Adv Appl Sci Res* 7:109–115

49. Feng-Yuan H (2012) Thermal properties and thermal degradation of cellulose tri-stearate (CTs). *Polymers* 4:1012–1024
50. Broido A (1969) A simple, sensitive graphical method of treating thermogravimetric analysis data. *J Polym Sci* 7:1761–1773
51. Coats AW, Redfern JP (1964) Kinetic parameters from thermogravimetric data. *Nature* 201:68–69
52. Shekh MI, Patel DM, Patel NN, Patel US, Patel KP, Patel RM (2018) Methacrylate copolymers and their composites with nano-CdS: synthesis, characterization, thermal behavior, and antimicrobial properties. *IJIC* 9:153–166
53. Shekh MI, Patel DM, Patel KP, Patel RM (2016) Electrospun nanofibers of poly(NPEMA-co.-CMPMA): used as heavy metal ion remover and water sanitizer. *Fiber Polym* 17:358–370
54. Shekh MI, Patel NN, Patel KP, Patel RM, Ray A (2017) Nano silver-embedded electrospun nanofiber of poly(4-chloro-3-methylphenyl methacrylate) use as water sanitizer. *Environ Sci Pollut Res* 24:5701–5716
55. Huang FY (2012) Thermal properties and thermal degradation of cellulose tri-stearate (CTs). *Polymers* 4:1012–1024
56. Moshiul Alam AKM, Beg MDH, Mina MF, Mamun AA, Bledzki AK (2015) Degradation and stability of green composites fabricated from oil palm empty fruit bunch fiber and polylactic acid: effect of fiber length. *J Compos Mater* 49:3103–3114
57. Ford JL (1999) Thermal analysis of hydroxypropylmethylcellulose and methylcellulose: powders, gels, matrix tablets. *Int J Pharm* 179:209–228
58. Picker KM, Hoag SW (2002) Characterization of the thermal properties of microcrystalline cellulose by modulated temperature differential scanning calorimetry. *J Pharm Sci* 91:342–349
59. Szczesniak L, Rachocki A (2008) Glass transition temperature and thermal decomposition of cellulose powder. *Cellulose* 15:445–451
60. Zhang X, Wang F, Keer LM (2015) Influence of surface modification on the microstructure and thermo-mechanical properties of bamboo fibers. *Materials* 8:6597–6608

Affiliations

Stefan Cichosz¹ · Anna Masek¹  · Korneliusz Wolski¹ · Marian Zaborski¹

✉ Anna Masek
anna.masek@p.lodz.pl

¹ Faculty of Chemistry, Institute of Polymer and Dye Technology, Lodz University of Technology, Stefanowskiego 12/16, 90-924 Lodz, Poland